Pathol. Oncol. Res. (2019) 25:1–9
DOI 10.1007/s12253-017-0305-4

ORIGINAL ARTICLE

MiR-490-5p Inhibits Hepatocellular Carcinoma Cell Proliferation, Migration and Invasion by Directly Regulating *ROBO1*

Weiqing Chen[1] · **Lijun Ye**[2] · **Dengcheng Wen**[1] · **Feihua Chen**[2]

Received: 8 June 2017 / Accepted: 1 September 2017 / Published online: 19 September 2017

Abstract Studies have investigated the effect of *ROBO1*. All the same, the relationship between miR-490-5p and *ROBO1*, and the underlying mechanism are still unclear. We aimed to study the effect of microRNA-490-5p (miR-490-5p) on hepatocellular carcinoma (HCC) cell proliferation, migration and invasion by directly regulating *ROBO1*. The expression of miR-490-5p and *ROBO1* in HCC tissues and cells were tested by RT-qPCR, and the Hep3B cells were selected for subsequent experiments. We confirmed the relationship between miR-490-5p and *ROBO1* by luciferase reporter system. The effects of miR-490-5p on cell proliferation, migration and invasion of Hep3B cells were assessed by MTT assay, colony formation assay, wound healing assay and transwell assay, respectively. Flow cytometry was employed to detect the influence of miR-490-5p on cell cycle and apoptosis of Hep3B cells. The expression of miR-490-5p was down-regulated, while *ROBO1* was up-regulated in HCC tissues and cells than the controls. MiR-490-5p can target *ROBO1*. MiR-490-5p inhibited cell proliferation, migration and invasion, but promoted cell apoptosis of Hep3B cells by inhibiting *ROBO1*. We confirmed that miR-490-5p could directly suppress *ROBO1*, which might be a potential mechanism in inhibiting HCC cell proliferation, migration and invasion.

Keywords Hepatocellular carcinoma · Hep3B · MiR-490-5p · *ROBO1*

✉ Feihua Chen
jxwang3188@163.com

[1] Department of General Surgery, The People's Hospital of Lin'an City, No 548 Yijing Street, Jincheng town, Lin'an City, Zhejiang Province 311300, China

[2] Department of Gynecology and Obstetrics, The People's Hospital of Lin'an City, Lin'an City, Zhejiang Province 311300, China

Introduction

Hepatocellular carcinoma (HCC) ranked the third-most leading cause of cancer-related deaths among the most popular tumors in humans all over the world [1]. Most of the HCC-associated deaths owe to secondary disease or metastatic progression among the estimated 1.4 million victims per annum. Although technologies for diagnosis and treatment advance swiftly over the years, HCC unfortunately remains highly fatal, for liver transplantation (LT) methods or hepatic resection therapies will not achieve beneficial effects on the majority of patients with small tumor or who live with well-compensated underlying liver diseases [2]. That's the reason why more comprehensive investigation in underlying molecular mechanism of HCC is needed.

MiRNA, a group of small single-stranded RNA that does not encode proteins, may function as oncogenes or tumor suppressors. It has been proved that miRNA could reduce gene expression in all cell types by binding to the 3′ untranslated region (3'UTR) of specific mRNA directly and therefore modulates mRNA degradation or inhibits translation [3, 4]. Previous studies have suggested that miR-490-5p is lower expressed in various tumor tissues such as colorectal cancer, bladder cancer and renal cell carcinoma [5, 6] than in normal tissues, indicating its potential tumor inhibitor role by suppressing cell proliferation, migration, and invasion [7].

Roundabout guidance receptor 1 (*ROBO1*) is a member of the neural cell adhesion molecule family of receptors [8]. It was reported that *ROBO1* was a tumor suppressor and it could be exploited as a molecular target to inhibit the progression of localized prostate cancer as well as treat metastasis in high-risk populations [9]. Moreover, Liu et al. found that miR-29a inhibits migration and invasion in part via direct inhibition of *ROBO1* in gastric cancer cells [10]. However, Hirotaka et al. reported that *ROBO1* was overexpressed in hepatocellular [11, 12].

The effect of miR-490-5p/*ROBO1* on the underlying mechanism is still unclear. Based on the reported functions of miR-490-5p and *ROBO1*, we made an endeavor to confirm the hypothesis that high level of miR-490-5p would reduce the expression of *ROBO1* and impact tumor progression. We employed advanced RT-qPCR, Western Blot and Dual Luciferase Reporter Gene Assay, MTT assay, Transwell Invasion Experiment and Flow Cytometry Analysis to investigate its effect on cell activities. This is the first reported study that elucidated the possible mechanism involving the miR-490-5p and *ROBO1* in human HCC which might enlighten us with a novel way of understanding HCC tumorigenesis.

Materials and Methods

Tissue Samples and Cell Culture

Both HCC tissues and adjacent tissues were obtained from 79 patients (51 males and 28 females) with HCC who were confirmed by experienced pathologists after liver surgery at hepatobiliary surgery center of Lin'an People's Hospital, the second Affiliate Hospital of Hangzhou Medical College from September 2013 to September 2015. No preoperative treatment had been conducted on patients. All fresh tissues were stored in −80 °C for subsequent experiments. All participants signed the informed consent. This study was conducted under the supervision of the ethics committee.

Human normal liver cell line L-02 and Human HCC cell lines Hep3B, SK-HEP-1, Huh-7, HepG2 (ATCC, Manassas, VA) were selected for experiments. All cell lines were cultured in DMEM containing 10% fetal bovine serum (FBS) (Gibco, Carlsbad, CA) at 5% CO_2, 37 °C.

Cell Transfection

MiR-490-5p mimics (synthesized by Shanghai GenePharma Co. Ltd) and *ROBO1*-cDNA (OriGene, USA) were transfected into Hep3B cells using Lipofectamine 2000 (Invitrogen, US). Patients were divided into the following groups: control, NC, miR-490-5p mimics, *ROBO1*-cDNA and miR-490-5p mimics + *ROBO1*-cDNA groups. After 48-h transfection, cells were harvested and used in subsequent experiments.

RT-qPCR

Total RNA was obtained from HCC tissues or cells by one step extraction method using Trizol agent (Invitrogen), and then reverse-transcribed to cDNAs using Primeseript TM RT kit (TaKaRa). The ABI7900 LightCycler (Roche) was selected to conduct the amplification of cDNAs. The primers used for RT-qPCR were shown in Table 1. U6 and GAPDH served as references, and the $2^{-\Delta\Delta C_t}$ method was used for the calculation of relative RNA expression.

Western Blotting

After transfection for 24 h, the total protein was extracted. The protein concentration was determined by using Braford method. Then proteins in samples were separated by sodium salt - polyacrylamide gel electrophoresis (SDS-PAGE), and subsequently transferred to a polyvinylidene fluoride (PVDF) membrane. After being blocked for 2 h using 5% skim milk, the membrane was incubated with primary antibodies against *ROBO1* and β-actin (1:200) (ABcam, UK) for 2 h. Finally, the membrane was incubated with HPR-conjugated secondary antibodies for another 2 h. Band signals were visualized using ECL. And β-actin served as the internal control.

MTT Assay

In the logarithmic growth phase, cells (1×10^6 cells/ml) were plated in 96-well plates. After incubated for 12, 24, 36, 48 and 60 h, cells in each well were overlaid with 10 μL 3-(4,5-dimethyl-2-thiazolyl)-2,5-diphenyl-2-H-tetrazolium bromide (MTT) solution for 4 h. Cells in each well were overlaid with 150 μL dimethyl sulphoxide (DMSO). The optical density (OD) of cells in different groups was detected at 12, 24, 36, 48 and 60 h after transfection using the microplate reader.

Colony Formation Assay

Cells were plated into 12-well plates (1×10^6 cells/well) and incubated for 2–3 weeks. The cells were allowed to proliferate till the colonies could be seen with naked eyes.

Table 1 Primers used in RT-qPCR

Primer	Sequence (5′ to 3′)
MiR-490-5p (F)	5′-CATGGATCTCCAGGTGG-3′
MiR-490-5p (R)	5′-TGGTGTCGTGGAGTCG-3′
U6 (F)	5′-CTCGCTTCGGCAGCACA-3′
U6 (R)	5′-AACGCTTCACGAATTTGCGT-3′
ROBO1 (F)	5′-GCATCGCTGGAAGTAGCCATACT-3’
ROBO1 (R)	5′-CATGAAATGGTGGGCTCAGGAT-3’
GAPDH (F)	5′-CCTGCCTCTACTGGCGCTGC-3’
GAPDH (R)	5′-GCAGTGGGGACACGGAAGGC-3’

F: forward primer; R: reverse primer

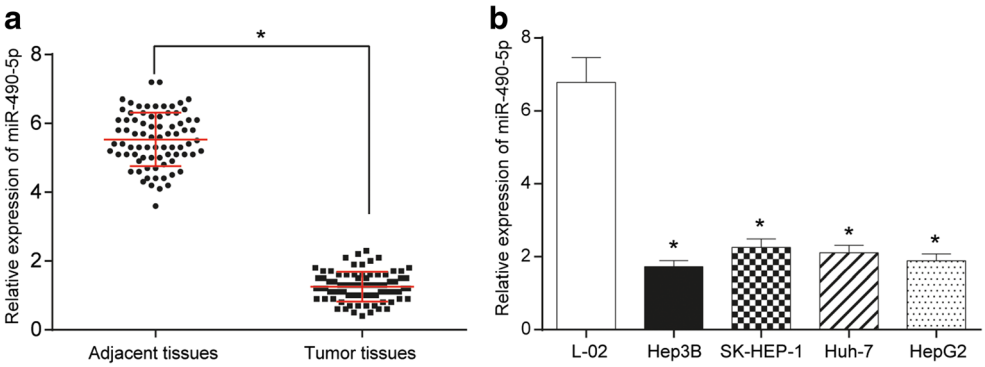

Fig. 1 The expression of miR-490-5p decreased in HCC tissues and cell lines. (**a**) MiR-490-5p expression decreased in HCC tissues compared with adjacent tissues. (**b**) MiR-490-5p expression decreased in HCC cell lines compared with normal liver cell line HL-7702. * $P < 0.05$, significantly different from the controls

The cells were then fixed in 4% paraformaldehyde and stained by Giemsa. The number of colonies was counted under a microscope.

Table 2 Association between clinicopathological characteristics of hepatocellular carcinoma patients and relative miR-490-5p expression

Characteristic	Relative miR-490-5p expression		*P* value
	Low ($n = 42$)	High ($n = 37$)	
Gender			0.481
Male	29	22	
Female	13	15	
Age (y)			0.264
≤ 60	16	19	
> 60	26	18	
Tumor grade			0.001*
G1	7	15	
G2	16	13	
G3	19	9	
Alcohol abuse			0.654
No	20	20	
Yes	22	17	
Lymph node metastasis			0.007*
No	12	22	
Yes	30	15	
TNM stage			0.073
I + II	15	21	
III + IV	27	16	
Tumor diameter (cm)			0.502
≤ 5	23	17	
> 5	19	20	
Serum AFP (ng/l)			0.655
≤ 400	18	18	
> 400	24	19	
Tumor recurrence			0.014*
No	14	23	
Yes	28	14	

The categorical data was compared by Chi-square tests. * $P < 0.05$ was statistically significant difference

Wound Healing Assay

After transfection for 48 h, each group of Hep3B cells was plated at a density of 5×10^5 cells per well in 6-well plates. When reached 90% confluences, cell monolayers were scratched with 50 μl pipette tips. The detached cells were washed away. At 0 h or 24 h after scratching, the cell monolayers were photographed with a phase-contrast inverted microscope.

Transwell Assay

Cells were plated in the upper chambers at a density of 5×10^4 cells per well. The membranes of upper chambers were precoated with 100 μL Matrigel (1 mg/mL). FBS was supplemented to the lower chambers as a stimulus. The membranes were fixed in 95% ethanol for 15–20 min and stained with hematoxylin for 10 min. Finally, random fields were selected to be observed under an inverted microscope.

Dual-Luciferase Reporter Gene Assay

The 3'UTR of *ROBO1* was amplified and cloned into PmirGLO eukaryotic expression vectors containing luciferase gene (System Biosciences) to construct pmirGLO-3-*ROBO1*-wt plasmids. The same method was used for the construction of the pmirGLO-3-*ROBO1*-mut plasmids by cloning mutated *ROBO1* 3'UTR to PmirGLO vectors.

The recombinant plasmid *ROBO1*-wt or *ROBO1*-mut and miR-490-5p mimics or NC were co-transfected to Hep3B cells with Lipofectamine 2000. At 48 h post-transfection, the relative luciferase activities were evaluated using Dual-Luciferase®Reporter Assay System (Promega).

Flow Cytometry Analysis

Each group of transfected cells was collected and centrifugated at 1000 rpm/min. Supernatant (cells) were suspended at 5×10^4 cells/ml. PBS solution, 1% BSA solution, 100 μL propidium iodide (PI) and 100 μL RNase A were added in sequence. After 30 min's incubation in the dark at 37 °C, the distribution of the cell cycle of Hep3B cells was detected by flow cytometry.

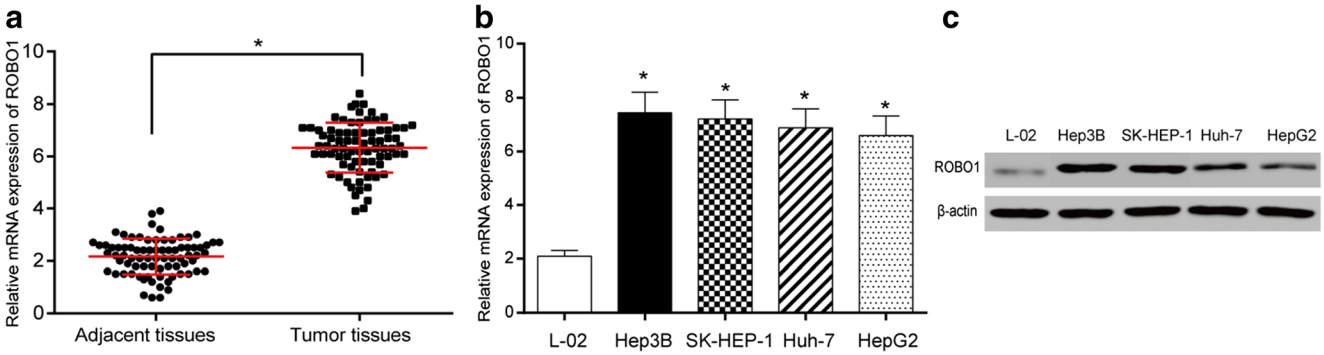

Fig. 2 The expression of *ROBO1* increased in HCC tissues and cell lines. (**a**) *ROBO1* expression increased in HCC tissues compared with adjacent tissues. (**b**) *ROBO1* expression increased in HCC cell lines compared to normal cell line HL-7702. (**c**) ROBO1 protein level in HCC cells increased compared with normal cells. * $P < 0.05$, significantly different from controls

For apoptosis analysis, after suspension, 100 μL Annexin V-FITC was added to the cell suspension and incubated for 15 min in the dark at 37 °C. Thereafter, the cell apoptosis was detected.

Statistical Analysis

Statistical analyses were accomplished using SPSS 21.0 (Chicago, Illinois, USA) and diagrams were conducted using GraphPad prism 6.0. The comparison between the two groups was conducted using t test, and the comparison among the multiple groups was conducted using one-way ANOVA. The significant difference was set at $P < 0.05$.

Results

MiR-490-5p Was Down-Regulated in HCC Tissues and Various HCC Cell Lines

The miR-490-5p level in HCC tissue samples and adjacent tissues were detected by RT-qPCR, and results showed that miR-490-5p in HCC tissues was remarkably down-regulated compared with adjacent tissues ($P < 0.05$, Fig. 1a). The miR-490-5p level was also detected in the normal liver cell line L-02 and various HCC cell lines, including Hep3B, SK-HEP-1, Huh-7 and HepG2, and the results suggested that the miR-490-5p expression was remarkably down-regulated in all HCC cell lines in comparison with normal cell line ($P < 0.05$, Fig. 1b).

A relative expression level of 1.3 of miR-490-5p in HCC was the cut-off point. 79 patients were then categorized into high miR-490-5p expression or low miR-490-5p group. The relationships among age, sex, alcohol abuse, lymph node metastasis, TNM stage, tumor diameter, tumor grade, serum alpha fetal protein (AFP) level, recurrence rate and miR-490-5p expression level were analyzed in 79 HCC patients. The results indicated that patients in the low miR-490-5p expression group had higher tumor grade, lymph node metastasis rate and recurrence rate at earlier TNM stage ($P < 0.05$). In addition, the miR-490-5p expression was not related to sex, age, alcohol abuse, tumor diameter and serum AFP level (Table 2, $P > 0.05$).

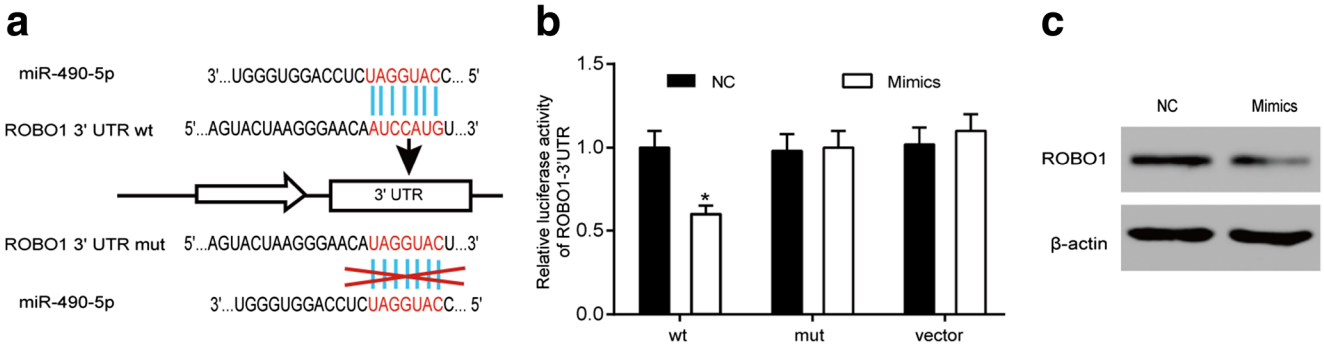

Fig. 3 *ROBO1* is directly targeted by miR-490-5p. (**a**) *ROBO1* mRNA is supposed to be a target of miR-490-5p with the binding sequence AUCCAUG. Multi-site mutation is used to mutate 7 nucleotides to construct *ROBO1*-mut 3'UTR. (**b**) Luciferase activity assay indicates that the binding sequence in *ROBO1* 3'UTR is necessary for the regulation by miR-490-5p. Hep3B cells transfected with miR-490-5p mimics and wild-type or mutated-type *ROBO1* 3'UTR (*ROBO1*-wt 3'UTR or *ROBO1*-mut 3'UTR) showed different luciferase intensities. The activity of mutated-type cannot be regulated by miR-490-5p. (**c**) ROBO1 protein level is suppressed by miR-490-5p mimics. * $P < 0.05$, significantly different from controls. NC: cells transfected with non-antisense oligomers. Mimics: cells transfected with miR-490-5p mimics

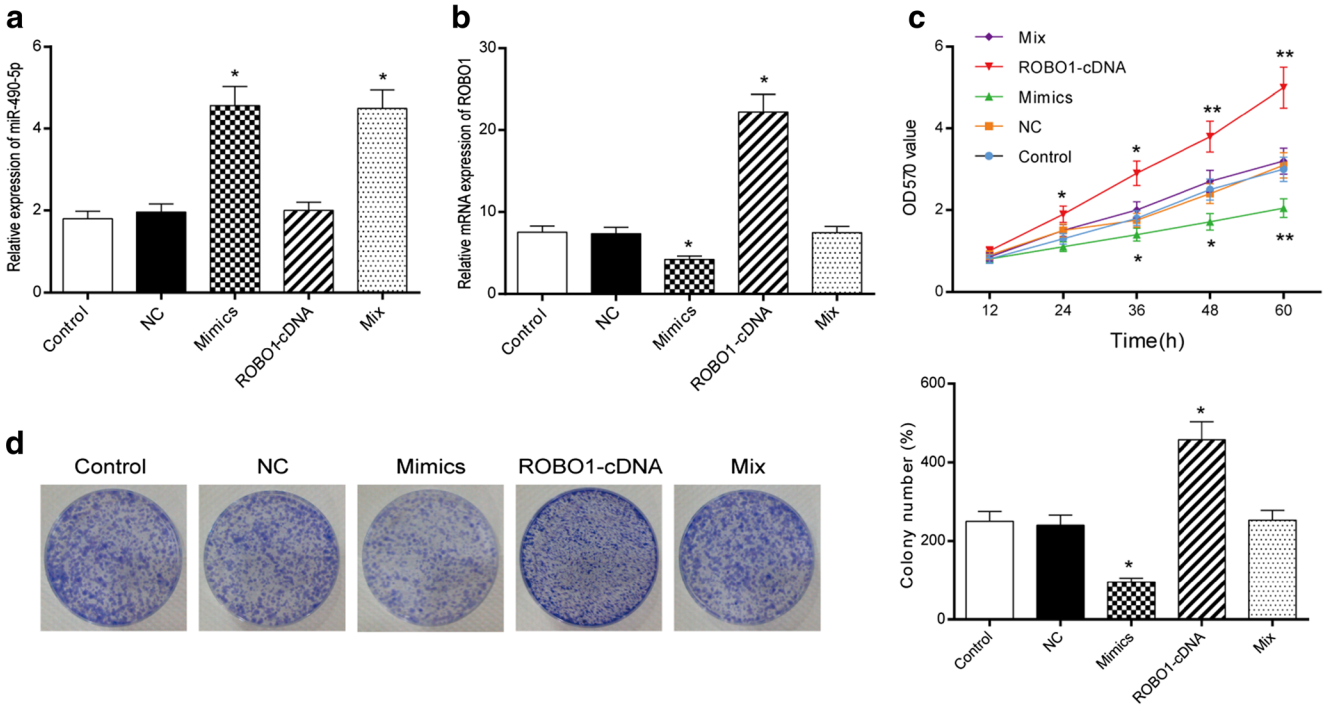

Fig. 4 MiR-490-5p inhibits the activity, proliferation, migration and invasion of HCC cells by suppressing *ROBO1*. (**a**) MiR-490-5p expression of cells in miR-490-5p mimics and miR-490-5p mimics + *ROBO1*-cDNA groups increased compared with control group. (**b**) *ROBO1* mRNA expression of cells increased in *ROBO1*-cDNA group but decreased in miR-490-5p mimics group compared with control group. (**c**) MTT assay result demonstrates that the overexpression of miR-490-5p inhibits Hep3B cell activity by suppressing *ROBO1*. (**d**) Colony formation assay results demonstrate that the overexpression of miR-490-5p inhibits Hep3B cell proliferation by suppressing *ROBO1*. * $P < 0.05$, significantly different from controls. Control: cells without transfection. NC: cells transfected with non-antisense oligomers. Mimics: cells transfected with miR-490-5p mimics. *ROBO1*-cDNA: cells transfected with *ROBO1* cDNA. Mix: cells co-transfected with miR-490-5p mimics and *ROBO1* cDNA

ROBO1 Was Up-Regulated in HCC Tissues and Cells

The expression of *ROBO1* mRNA in HCC tissues and adjacent tissues was determined by RT-qPCR. The results displayed a notably higher level of *ROBO1* mRNA in HCC tissues than in adjacent tissues ($P < 0.05$, Fig. 2a). The *ROBO1* mRNA level was also detected in the normal liver cell line L-02 and various HCC cell lines, including Hep3B, SK-HEP-1, Huh-7 and HepG2, and the results suggested that the *ROBO1* mRNA expression was remarkably higher in HCC cells compared with normal cells ($P < 0.05$, Fig. 2b). The protein expression of *ROBO1* was assessed with western blot, and the results displayed a notable up-regulation of *ROBO1* protein level in HCC cells compared with the normal cell line ($P < 0.05$, Fig. 2c). The following experiments were conducted in Hep3B cells in which ROBO1 had the highest level.

ROBO1 Was the Target of miR-490-5p

The predicted binding site of miR-490-5p retrieved from TargetScan Human 7.0 database on *ROBO1* 3'TUR was illustrated in Fig. 3a. To verify the above speculation, we constructed wild-type and mutated-type *ROBO1* luciferase reporter gene vectors, which were co-transfected with miR-490-5p mimics into the cells. The results suggested that the luciferase activity of cells transfected with *ROBO1*-wt 3'UTR and miR-490-5p mimics was suppressed dramatically ($P < 0.05$), while that of cells transfected with *ROBO1*-mut 3'UTR and miR-490-5p mimics did not alter substantially compared with the controls, respectively ($P > 0.05$, Fig. 3b), showing that miR-490-5p could directly target *ROBO1* mRNA and reduce its stabilization or translation.

The depressing effect of miR-490-5p on *ROBO1* was also evaluated at translational level. *ROBO1* protein expression was severely down-regulated in Hep3B cells transfected with miR-490-5p mimics compared with NC group ($P < 0.05$, Fig. 3c), showing that the over-expression of miR-490-5p has inhibitory effect on *ROBO1*.

MiR-490-5p Suppressed HCC Cell Proliferation by Restraining ROBO1

After transfection, the expression levels of miR-490-5p and *ROBO1* in each group were detected by RT-qPCR to verify the efficiency of cell transfection. MiR-490-5p expression of miR-490-5p mimics and miR-490-5p mimics + *ROBO1*-cDNA groups increased significantly compared with the control group ($P < 0.05$, Fig. 4a). *ROBO1* mRNA expression of *ROBO1*-cDNA group increased, while that of miR-490-5p mimics group

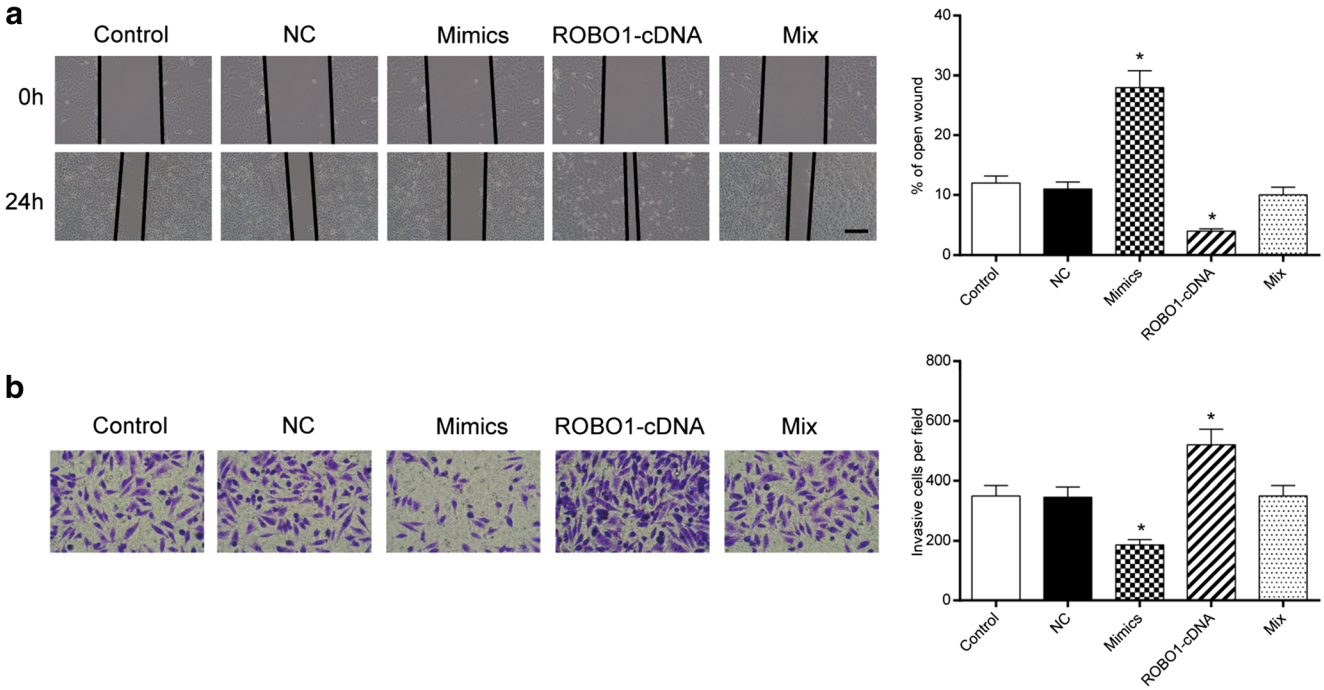

Fig. 5 MiR-490-5p inhibited HCC cell migration and invasion by suppressing *ROBO1*. (**a**) Wound healing assay results demonstrate that the overexpression of miR-490-5p inhibits Hep3B cell migration by suppressing *ROBO1*. (**b**) Transwell assay results demonstrate that the over-expression of miR-490-5p inhibits Hep3B cell invasion by suppressing *ROBO1* (×400). * $P < 0.05$, significantly different from controls. Control: cells without transfection. NC: cells transfected with non-antisense oligomers. Mimics: cells transfected with miR-490-5p mimics. *ROBO1*-cDNA: cells transfected with *ROBO1* cDNA. Mix: cells co-transfected with miR-490-5p mimics and *ROBO1* cDNA

decreased compared with the control group ($P < 0.05$, Fig. 4b). Besides, the miR-490-5p expression of cells in *ROBO1*-cDNA group did not show significant difference from the control and the NC group. And there was no remarkable difference of *ROBO1* expression among the control, the NC and the miR-490-5p mimics + *ROBO1*-cDNA groups ($P > 0.05$).

MTT results displayed that there was no notable distinction in cell viability among the groups after 24 h transfection ($P > 0.05$). After being transfected for 36 h, cells of miR-490-5p mimics group had significant lower viability while those of *ROBO1*-cDNA group had significant higher viability than those of control group ($P < 0.05$). After being transfected for 60 h, the cells in the miR-490-5p mimics and *ROBO1*-cDNA groups showed further notable differences in viability from those in control group ($P < 0.01$, Fig. 4c). MiR-490-5p mimics + *ROBO1*-cDNA group was not significantly different from control groups in terms of cell viability at any indicating time point ($P > 0.05$). These results demonstrate that the overexpression of miR-490-5p in Hep3B cell could suppress cell viability, while the overexpression of *ROBO1* could enhance the activity of HCC cells. Additionally, the overexpression of *ROBO1* could counteract the inhibition of miR-490-5p on cell viability.

Similar with MTT results, cells in miR-490-5p mimics group formed significant fewer colonies, while those in *ROBO1*-cDNA group formed more colonies than those in control group ($P < 0.05$, Fig. 4d). There was no significant difference between miR-490-5p mimics + *ROBO1*-cDNA and control group ($P > 0.05$), indicating that the miR-490-5p over-expression inhibited Hep3B cell proliferation, while *ROBO1* over-expression promoted Hep3B cell proliferation, and *ROBO1* over-expression counteracted the suppression effect of miR-490-5p on cell proliferation.

MiR-490-5p Inhibited HCC Cell Migration and Invasion by Suppressing ROBO1

The results of wound healing assay demonstrated that cells in miR-490-5p mimics group had lower cell migration rate, while cells in *ROBO1*-cDNA group had higher cell migration rate than those in control group ($P < 0.05$, Fig. 5a). No significant differences were found between miR-490-5p mimics + *ROBO1*-cDNA and control group in terms of cell migration rate ($P > 0.05$).

Results of Transwell assay indicated that cells in miR-490-5p mimics group had less severe cell invasiveness, while those in *ROBO1*-cDNA group had more severe cell invasiveness than those in control group ($P < 0.05$, Fig. 5b). No significant differences were detected among control group, NC group and miR-490-5p mimics + *ROBO1*-cDNAgroup ($P > 0.05$).

These results confirmed that the miR-490-5p over-expression inhibited Hep3B cell migration and invasion, while *ROBO1* over-expression promoted Hep3B cell migration and invasion, and the over-expression of *ROBO1* could counteract the inhibitory effects of miR-490-5p on cell migration and invasion.

MiR-490-5p Regulated Cell Cycle of HCC Cells by Inhibiting ROBO1

The percentage of cells arrested in G0/G1 phase increased significantly, while the percentage of cells entering the S and G2/M phases decreased substantially in the miR-490-5p mimics group compared with the control group ($P < 0.05$). On the other hand, the percentage of cells arrested in G0/G1 phase decreased in *ROBO1*-cDNA group, while the percentage of cells entering S phase increased compared with control group ($P < 0.05$, Figs. 6a and c). Cell cycle of cells transfected in NC and miR-490-5p mimics + *ROBO1*-cDNA was not significantly different from those in control group ($P > 0.05$). These results suggested that miR-490-5p in Hep3B cells could arrest cell cycle and inhibit cell mitosis by suppressing *ROBO1*.

MiR-490-5p Regulated Cell Apoptosis of HCC Cells by Inhibiting ROBO1

The miR-490-5p-mediated cell apoptosis was detected using flow cytometry. Hep3B cells in miR-490-5p mimics group had higher cell apoptosis rate, while those in *ROBO1*-cDNA group had lower cell apoptosis rate compared with those in

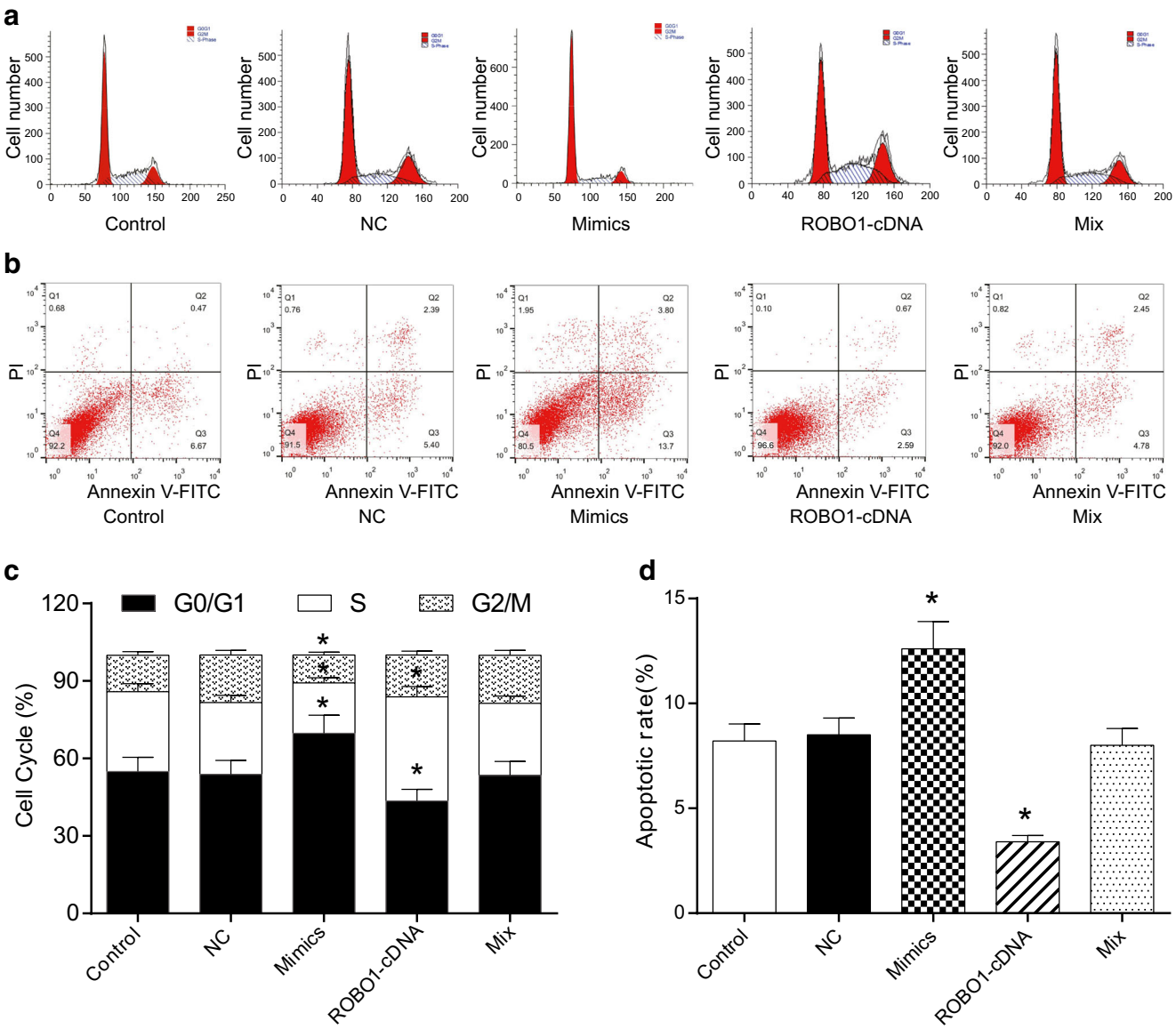

Fig. 6 MiR-490-5p arrests Hep3B cell cycle and promotes cell apoptosis by suppressing *ROBO1*. (**a**)(**c**) Over-expression of miR-490-5p increases the ratio of Hep3B cells in G0/G1 phase, while decreases the proportion of Hep3B cells in S and G2/M phases. Over-expression of *ROBO1* has opposite effects. (**b**)(**d**) The results of cell apoptosis assay detected by flow cytometry suggest that overexpression of miR-490-5p could facilitate cell apoptosis by suppressing *ROBO1*. * $P < 0.05$, significantly different from controls. Control: cells without transfection. NC: cells transfected with non-antisense oligomers. Mimics: cells transfected with miR-490-5p mimics. *ROBO1*-cDNA: cells transfected with *ROBO1* cDNA. Mix: cells co-transfected with miR-490-5p mimics and *ROBO1* cDNA

control group ($P < 0.05$, Figs. 6b and d). Cell apoptosis in the NC and miR-490-5p mimics + *ROBO1*-cDNA groups did not significantly differ from that in control group ($P > 0.05$). These results suggested that miR-490-5p in Hep3B cells could promote Hep3B cell apoptosis by suppressing *ROBO1*.

Discussion

In the present study, we explored the expression of miR-490-5p and *ROBO1* in hepatic tissues and cells. We also investigated the effects of miR-490-5p and *ROBO1* on a series of hepatic cell activities. In addition, we confirmed the direct binding relationship between miR-490-5p and *ROBO1*. Our findings revealed the possible mechanism of hepatocellular carcinogenesis.

A battery of miRNAs has been reported to be significantly different in tumorous tissues from in normal tissues. For instance, miR-551a, miR-483-5p, miR-124 and miR-26 (a) were reported to be deregulated in hepatocellular carcinoma (HCC) [13–18]. On the other hand, miR-490-3p has been reported to be an independent indicator for Ewing's sarcoma [19]. Substantial down-regulation of miR-490-3p in human gastric cancer tissues was confirmed by Shen et al. [20]. Similarly, miR-490-3p has been reported to be lower-expressed in endometrial cancer tissues than in normal endometrial tissues [20, 21]. Not surprisingly, miR-490-3p was found substantially down-regulated among the top deregulated miRNAs in HCC as well [22]. MiR-490-5p, on the other hand, showed higher expression level in human bladder cancer tissues and cells than non-cancerous tissues and cells [5], but was also found the most strongly down-regulated ($\log_2$Ratio = − 5.79794) in human bladder urothelial carcinoma by deep sequencing [23, 24]. Besides, miR-490-5p together with a broad spectrum of other miRNAs were found significantly up-regulated in six human malignant cell lines (squamous cell carcinoma of the head and neck, human brain tumours) following irradiation than in those without irradiation treatment [25, 26]. In addition, miR-490-5p was also found down-regulated by over 2-fold change before and after chondrogenesis [27]. However, to our knowledge, little has been done to clarify the expression of miR-490-5p in HCC or any other cancers. We herein detected the relative expression of miR-490-5p in liver tissues and cells, and we found that miR-490-5p was severely down-regulated in tumorous tissues and cell lines, indicating its tumour suppressor role in HCC. In addition, this aberrant expression of miR-490-5p is a possible biomarker for HCC.

The target relationship between miR-490-5p and *ROBO1* has not been reported in any cancerous cells yet. We, however, in this study, verified that miR-490-5p directly bound to *ROBO1* 3'UTR and regulated Hep3B cell activities. *ROBO1* functions in migration, invasion and its aberrant expression regulate the development of major axon tracts and interneuron migration in the forebrain [3]. In our study, *ROBO1* was found over-expressed in HCC tissues and cell lines, suggesting its possible tumour facilitator role. Consistently, *ROBO1* was reported to be involved in the high expression in human liver cancer [11]. Our experiment of western blot verified this point. Moreover, *ROBO1* was negatively regulated by miR-218 in gastric cancer. The activation of the Slit-Robo1 pathway through the interaction between Robo1 and Slit2 could trigger tumor metastasis [28–30]. Besides, miR-490-5p could significantly suppress the proliferation and mitosis of human bladder cancer cell lines by directly binding to c-Fos, a proto-oncogene [5]. Thus, we believe that miR-490-5p may inhibit the propagation, viability, migration, and invasion and induce cell apoptosis by directly targeting *ROBO1*. Whereas the activation of miR-490-5p could inhibit cell proliferation, the repression of *ROBO1* with miR-490-5p could possiblely lead to the enhancement of cell proliferation.

However, to validate whether miR-490-5p/*ROBO1* interplay affects HCC cell apoptosis, migration and invasion by participating in specific signaling pathways, further researches need to be done to discover the involvement of the pathways and their relation with cell apoptosis, migration and invasion.

Collectively, we explored the expression of miR-490-5p and *ROBO1* in human HCC tissues and cell lines. Besides, we confirmed the target relationship between miR-490-5p and *ROBO1*. In addition, we investigated the possible molecular mechanism by which miR-490-5p/*ROBO1* interplay affects HCC cell apoptosis, proliferation, migration and invasion etc. Our findings also explained the possible clinical significance of miR-490-5p/*ROBO1* interplay in HCC.

Compliance with Ethical Standards

Conflict of Interest The authors declare that they have no conflict of interest.

References

1. Chuang KH, Whitney-Miller CL, Chu CY, Zhou Z, Dokus MK, Schmit S, Barry CT (2015) MicroRNA-494 is a master epigenetic regulator of multiple invasion-suppressor microRNAs by targeting ten eleven translocation 1 in invasive human hepatocellular carcinoma tumors. Hepatology (Baltimore, Md) 62(2):466–480. https://doi.org/10.1002/hep.27816
2. Allen MD, Luong P, Hudson C, Leyton J, Delage B, Ghazaly E, Cutts R, Yuan M, Syed N, Lo Nigro C, Lattanzio L, Chmielewska-Kassassir M, Tomlinson I, Roylance R, Whitaker HC, Warren AY, Neal D, Frezza C, Beltran L, Jones LJ, Chelala C, Wu BW, Bomalaski JS, Jackson RC, Lu YJ, Crook T, Lemoine NR, Mather S, Foster J, Sosabowski J, Avril N, Li CF, Szlosarek PW (2014) Prognostic and therapeutic impact of argininosuccinate synthetase 1 control in bladder cancer as monitored longitudinally by PET imaging. Cancer Res 74(3):896–907. https://doi.org/10.1158/0008-5472.CAN-13-1702

3. Chinn GA, Hirokawa KE, Chuang TM, Urbina C, Patel F, Fong J, Funatsu N, Monuki ES (2015) Agenesis of the corpus callosum due to defective glial wedge formation in Lhx2 mutant mice. Cereb Cortex 25(9):2707–2718. https://doi.org/10.1093/cercor/bhu067
4. Kim SH, Lee KH, Kim DY, Kwak E, Kim S, Kim KT (2015) Rhythmic control of mRNA stability modulates circadian amplitude of mouse Period3 mRNA. J Neurochem 132(6):642–656. https://doi.org/10.1111/jnc.13027
5. Li S, Xu X, Xu X, Hu Z, Wu J, Zhu Y, Chen H, Mao Y, Lin Y, Luo J, Zheng X, Xie L (2013) MicroRNA-490-5p inhibits proliferation of bladder cancer by targeting c-Fos. Biochem Biophys Res Commun 441(4):976–981. https://doi.org/10.1016/j.bbrc.2013.11.006
6. Chen K, Zeng J, Tang K, Xiao H, Hu J, Huang C, Yao W, Yu G, Xiao W, Guan W, Guo X, Xu H, Ye Z (2016) miR-490-5p suppresses tumour growth in renal cell carcinoma through targeting PIK3CA. Biol Cell 108(2):41–50. https://doi.org/10.1111/boc.201500033
7. Zhang LY, Liu M, Li X, Tang H (2013) miR-490-3p modulates cell growth and epithelial to mesenchymal transition of hepatocellular carcinoma cells by targeting endoplasmic reticulum-Golgi intermediate compartment protein 3 (ERGIC3). J Biol Chem 288(6):4035–4047. https://doi.org/10.1074/jbc.M112.410506
8. Saini V, Loers G, Kaur G, Schachner M, Jakovcevski I (2016) Impact of neural cell adhesion molecule deletion on regeneration after mouse spinal cord injury. Eur J Neurosci 44(1):1734–1746. https://doi.org/10.1111/ejn.13271
9. Parray A, Siddique HR, Kuriger JK, Mishra SK, Rhim JS, Nelson HH, Aburatani H, Konety BR, Koochekpour S, Saleem M (2014) ROBO1, A tumor suppressor and critical molecular barrier for localized tumor cells to acquire invasive phenotype: study in African-American and Caucasian prostate cancer models. Int J Cancer 135(11):2493–2506. https://doi.org/10.1002/ijc.28919
10. Liu X, Cai J, Sun Y, Gong R, Sun D, Zhong X, Jiang S, He X, Bao E, Yang L, Li Y (2015) MicroRNA-29a inhibits cell migration and invasion via targeting roundabout homolog 1 in gastric cancer cells. Mol Med Rep 12(3):3944–3950. https://doi.org/10.3892/mmr.2015.3817
11. Ito H, Funahashi S, Yamauchi N, Shibahara J, Midorikawa Y, Kawai S, Kinoshita Y, Watanabe A, Hippo Y, Ohtomo T, Iwanari H, Nakajima A, Makuuchi M, Fukayama M, Hirata Y, Hamakubo T, Kodama T, Tsuchiya M, Aburatani H (2006) Identification of ROBO1 as a novel hepatocellular carcinoma antigen and a potential therapeutic and diagnostic target. Clin Cancer Res 12(11 Pt 1):3257–3264. https://doi.org/10.1158/1078-0432.CCR-05-2787
12. Ao JY, Chai ZT, Zhang YY, Zhu XD, Kong LQ, Zhang N, Ye BG, Cai H, Gao DM, Sun HC (2015) Robo1 Promotes angiogenesis in hepatocellular carcinoma through the rho family of guanosine triphosphatases' signaling pathway. Tumour Biol 36(11):8413–8424. https://doi.org/10.1007/s13277-015-3601-1
13. Sullivan WJ, Christofk HR (2015) The metabolic milieu of metastases. Cell 160(3):363–364. https://doi.org/10.1016/j.cell.2015.01.023
14. Viswanathan SR, Powers JT, Einhorn W, Hoshida Y, Ng TL, Toffanin S, O'Sullivan M, Lu J, Phillips LA, Lockhart VL, Shah SP, Tanwar PS, Mermel CH, Beroukhim R, Azam M, Teixeira J, Meyerson M, Hughes TP, Llovet JM, Radich J, Mullighan CG, Golub TR, Sorensen PH, Daley GQ (2009) Lin28 Promotes transformation and is associated with advanced human malignancies. Nat Genet 41(7):843–848. https://doi.org/10.1038/ng.392
15. Loo JM, Scherl A, Nguyen A, Man FY, Weinberg E, Zeng Z, Saltz L, Paty PB, Tavazoie SF (2015) Extracellular metabolic energetics can promote cancer progression. Cell 160(3):393–406. https://doi.org/10.1016/j.cell.2014.12.018
16. Hatziapostolou M, Polytarchou C, Aggelidou E, Drakaki A, Poultsides GA, Jaeger SA, Ogata H, Karin M, Struhl K, Hadzopoulou-Cladaras M, Iliopoulos D (2011) An HNF4alpha-miRNA inflammatory feedback circuit regulates hepatocellular oncogenesis. Cell 147(6):1233–1247. https://doi.org/10.1016/j.cell.2011.10.043
17. Kota J, Chivukula RR, O'Donnell KA, Wentzel EA, Montgomery CL, Hwang HW, Chang TC, Vivekanandan P, Torbenson M, Clark KR, Mendell JR, Mendell JT (2009) Therapeutic microRNA delivery suppresses tumorigenesis in a murine liver cancer model. Cell 137(6):1005–1017. https://doi.org/10.1016/j.cell.2009.04.021
18. Ji J, Shi J, Budhu A, Yu Z, Forgues M, Roessler S, Ambs S, Chen Y, Meltzer PS, Croce CM, Qin LX, Man K, Lo CM, Lee J, Ng IO, Fan J, Tang ZY, Sun HC, Wang XW (2009) MicroRNA expression, survival, and response to interferon in liver cancer. N Engl J Med 361(15):1437–1447. https://doi.org/10.1056/NEJMoa0901282
19. Nakatani F, Ferracin M, Manara MC, Ventura S, Del Monaco V, Ferrari S, Alberghini M, Grilli A, Knuutila S, Schaefer KL, Mattia G, Negrini M, Picci P, Serra M, Scotlandi K (2012) miR-34a predicts survival of Ewing's sarcoma patients and directly influences cell chemo-sensitivity and malignancy. J Pathol 226(5):796–805. https://doi.org/10.1002/path.3007
20. Shen J, Xiao Z, Wu WK, Wang MH, To KF, Chen Y, Yang W, Li MS, Shin VY, Tong JH, Kang W, Zhang L, Li M, Wang L, Lu L, Chan RL, Wong SH, Yu J, Chan MT, Chan FK, Sung JJ, Cheng AS, Cho CH (2015) Epigenetic silencing of miR-490-3p reactivates the chromatin remodeler SMARCD1 to promote helicobacter pylori-induced gastric carcinogenesis. Cancer Res 75(4):754–765. https://doi.org/10.1158/0008-5472.CAN-14-1301
21. Sun KX, Chen Y, Chen S, Liu BL, Feng MX, Zong ZH, Zhao Y (2016) The correlation between microRNA490-3p and TGFalpha in endometrial carcinoma tumorigenesis and progression. Oncotarget 7(8):9236–9249. 10.18632/Oncotarget.7061
22. Wojcicka A, Swierniak M, Kornasiewicz O, Gierlikowski W, Maciag M, Kolanowska M, Kotlarek M, Gornicka B, Koperski L, Niewinski G, Krawczyk M, Jazdzewski K (2014) Next generation sequencing reveals microRNA isoforms in liver cirrhosis and hepatocellular carcinoma. Int J Biochem Cell Biol 53:208–217. https://doi.org/10.1016/j.biocel.2014.05.020
23. Han Y, Chen J, Zhao X, Liang C, Wang Y, Sun L, Jiang Z, Zhang Z, Yang R, Chen J, Li Z, Tang A, Li X, Ye J, Guan Z, Gui Y, Cai Z (2011) MicroRNA expression signatures of bladder cancer revealed by deep sequencing. PLoS One 6(3):e18286. https://doi.org/10.1371/journal.pone.0018286
24. Xu S, Gu G, Ni Q, Li N, Yu K, Li X, Liu C (2015) The expression of AEG-1 and cyclin D1 in human bladder urothelial carcinoma and their clinicopathological significance. Int J Clin Exp Med 8(11):21222–21228
25. Niemoeller OM, Niyazi M, Corradini S, Zehentmayr F, Li M, Lauber K, Belka C (2011) MicroRNA expression profiles in human cancer cells after ionizing radiation. Radiat Oncol 6:29. https://doi.org/10.1186/1748-717X-6-29
26. Pearson GR, Orr T, Rabin H, Cicmanec J, Ablashi D, Armstrong G (1973) Antibody patterns to herpesvirus saimiri-induced antigens in owl monkeys. J Natl Cancer Inst 51(6):1939–1943
27. Zhang Z, Kang Y, Zhang Z, Zhang H, Duan X, Liu J, Li X, Liao W (2012) Expression of microRNAs during chondrogenesis of human adipose-derived stem cells. Osteoarthr Cartil 20(12):1638–1646. https://doi.org/10.1016/j.joca.2012.08.024
28. Tie J, Pan Y, Zhao L, Wu K, Liu J, Sun S, Guo X, Wang B, Gang Y, Zhang Y, Li Q, Qiao T, Zhao Q, Nie Y, Fan D (2010) MiR-218 inhibits invasion and metastasis of gastric cancer by targeting the Robo1 receptor. PLoS Genet 6(3):e1000879. https://doi.org/10.1371/journal.pgen.1000879
29. Tang W, Tang J, He J, Zhou Z, Qin Y, Qin J, Li B, Xu X, Geng Q, Jiang W, Wu W, Wang X, Xia Y (2015) SLIT2/ROBO1-miR-218-1-RET/PLAG1: a new disease pathway involved in Hirschsprung's disease. J Cell Mol Med 19(6):1197–1207. https://doi.org/10.1111/jcmm.12454
30. Gara RK, Kumari S, Ganju A, Yallapu MM, Jaggi M, Chauhan SC (2015) Slit/Robo pathway: a promising therapeutic target for cancer. Drug Discov Today 20(1):156–164. https://doi.org/10.1016/j.drudis.2014.09.008